HDAC6/aggresome processing pathway importance for inflammasome formation is context dependent

Longlong Wang, Shihua Shi, Adeline Unterreiner, Ronan Kapetanovic, Sucheta Ghosh, Jacint Sanchez, Selma Aslani, Yuan Xiong, Chi-Lin Hsu, Katherine A Donovan, et al.

Journal Pre-proof

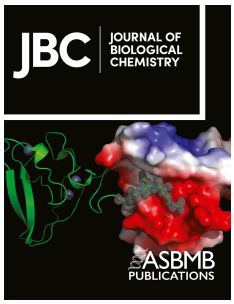

HDAC6/aggresome processing pathway importance for inflammasome formation is context dependent

Longlong Wang, Shihua Shi, Adeline Unterreiner, Ronan Kapetanovic, Sucheta Ghosh, Jacint Sanchez, Selma Aslani, Yuan Xiong, Chi-Lin Hsu, Katherine A. Donovan, Christopher J. Farady, Eric S. Fischer, Frédéric Bornancin, Patrick Matthias

PII: S0021-9258(24)00014-0

DOI: https://doi.org/10.1016/j.jbc.2024.105638

Reference: JBC 105638

To appear in: *Journal of Biological Chemistry*

Received Date: 21 August 2023

Revised Date: 19 December 2023

Accepted Date: 31 December 2023

Please cite this article as: Wang L, Shi S, Unterreiner A, Kapetanovic R, Ghosh S, Sanchez J, Aslani S, Xiong Y, Hsu CL, Donovan KA, Farady CJ, Fischer ES, Bornancin F, Matthias P, HDAC6/aggresome processing pathway importance for inflammasome formation is context dependent, *Journal of Biological Chemistry* (2024), doi: https://doi.org/10.1016/j.jbc.2024.105638.

HDAC6/aggresome processing pathway importance for inflammasome formation is context dependent

Longlong Wang[a*], Shihua Shi[a], Adeline Unterreiner[b], Ronan Kapetanovic[a,c], Sucheta Ghosh[a,d], Jacint Sanchez[a], Selma Aslani[b], Yuan Xiong[e,f], Chi-Lin Hsu[e,f], Katherine A. Donovan[e,f], Christopher J. Farady[b], Eric S. Fischer[e,f], Frédéric Bornancin[b], & Patrick Matthias[a, d*]

Affiliations:

[a] Friedrich Miescher Institute for Biomedical Research, 4058 Basel, Switzerland

[b] Novartis Institutes for Biomedical Research, 4056 Basel Switzerland

[c] present address: INRAE, Université de Tours, ISP, Nouzilly, France

[d] Faculty of Sciences, University of Basel, 4031 Basel, Switzerland

[e] Department of Cancer Biology, Dana Farber Cancer Institute, Boston, MA 02215, United States

[f] Department of Biological Chemistry and Molecular Pharmacology, Harvard Medical School, Boston, MA 02115, United States

*Corresponding authors

PM Orcid ID: 0000-0002-3927-1452
LW Orcid ID: 0000-0001-5279-1885
SS Orcid ID: 0000-0001-6475-2349
RK Orcid ID: 0000-0002-2908-1014
FB Orcid ID: 0000-0002-0152-6720
ESF Orcid ID: 0000-0001-7337-6306
CJF Orcid ID: 0000-0002-3607-9721
KAD Orcid ID: 0000-0002-8539-5106
YX Orcid ID: 0000-0002-2211-8267

Running title: HDAC6 and inflammasome activation

Keywords: Inflammasome, HDAC6, degrader, inhibitors, DARPin, interleukin

Abstract

The inflammasome is a large multiprotein complex that assembles in the cell cytoplasm in response to stress or pathogenic infection. Its primary function is to defend the cell and promote the secretion of pro-inflammatory cytokines, including IL-1β and IL-18. Previous research has shown that in immortalized bone marrow-derived macrophages (iBMDMs) inflammasome assembly is dependent on the deacetylase HDAC6 and the aggresome processing pathway (APP), a cellular pathway involved in the disposal of misfolded proteins. Here we used primary BMDMs from mice in which HDAC6 is ablated or impaired and found that inflammasome activation was largely normal. We also used human peripheral blood mononuclear cells and monocytes cell lines expressing a synthetic protein blocking the HDAC6-ubiquitin interaction and impairing the APP and found that inflammasome activation was moderately affected. Finally, we used a novel HDAC6 degrader and showed that inflammasome activation was partially impaired in human macrophage cell lines with depleted HDAC6. Our results therefore show that HDAC6 importance in inflammasome activation is context dependent.

Introduction

The inflammasome is a critical protein complex involved in the body's immune response (1). When activated, the inflammasome releases the pro-inflammatory cytokines interleukin (IL)-1β and IL-18 , which can result in tissue damage and cell death through pyroptosis (2). Several sensor proteins can nucleate inflammasome assembly, including NLRP and NLRC subfamilies, AIM2, and pyrin. Among these, the NLRP3 inflammasome, which is key for sterile inflammation has been extensively studied (3). Activation of the NLRP3 inflammasome often requires a transcriptional priming step to upregulate the inflammasome components such as NLRP3 and IL-1β. Priming agents, e.g., bacterial lipopolysaccharide (LPS), tumor necrosis factor (TNF) or phorbol 12-myristate 13-acetate (PMA), also trigger critical post-translational modifications that sensitize the inflammasome components to subsequent activation. Various stimuli, including the pore-forming toxin nigericin, adenosine-triphosphate (ATP) (4) and monosodium urate crystals (MSU) (5) can stimulate NLRP3 inflammasome assembly, leading to pro-caspase 1 activation, followed by cleavage and release of IL-1β (3). Aberrant inflammasome activity has been linked to many diseases (3), and a detailed understanding of the inflammasome's activation process is crucial for the development of potential treatments for diseases related to inflammation and immune responses.

The aggresome processing pathway (APP) is a stress-response pathway that is activated when misfolded proteins accumulate; it promotes the formation of the aggresome, a deposit of misfolded and ubiquitinated proteins near the microtubule-organizing center (MTOC), which is subsequently eliminated by autophagy (6). An essential component of the APP is the lysine deacetylase HDAC6 (7), an atypical enzyme with two catalytic domains and a zinc finger domain (ZnF-UbP, hereafter ZnF) binding the small protein ubiquitin (Ub). HDAC6 has been implicated in diverse normal or pathological cellular processes, such as stress response (e.g. APP and stress granules formation) (8), cancer (9), inflammation and viral infection (10). Depending on the situation, the catalytic domains (regulating acetylation levels of the relevant substrate) and/or the ZnF domain (recruiting Ub) are important for optimal HDAC6 function. In its role in the APP, HDAC6 acts as an adapter protein that promotes

transport of ubiquitinated misfolded proteins by dynein motor proteins along the MTs towards the MTOC. For this, both the ZnF and the catalytic domains are critical.

It has recently been proposed that formation of the NLRP3 and pyrin inflammasomes takes place near the MTOC and uses components of the APP machinery and that consequently inflammasome formation is impaired in cells lacking HDAC6 or expressing HDAC6 with a mutated ZnF domain (11). Furthermore, the lysosomal Ragulator complex was recently reported to activate the NLRP3 inflammasome in vivo via HDAC6 (12). Given the apparent similarity between inflammasome formation and APP – in both cases assembly of a complex near the MTOC – it is plausible that HDAC6 could be involved in both pathways, but to define the absolute requirement of HDAC6 in inflammasome activation, a robust profiling of orthogonal methods needs to be tested in different settings. Here we have examined the importance of HDAC6 for inflammasome activation in different cellular systems, including primary mouse cells (BMDMs), peripheral blood mononuclear cells (PMBCs) and human cell lines and manipulated HDAC6 levels through different approaches. Under the conditions tested, we found that the activation of NLRP3 was only partially dependent on HDAC6.

Results

NLRP3 inflammasome is activated efficiently in HDAC6 KO and ZnF^m BMDMs

Previous work identified the role for HDAC6 in inflammasome activation in immortalized bone marrow-derived macrophages (iBMDMs) (11). To avoid alterations in transcriptome and other cellular processes associated with establishment of an immortalized cell line, we first used primary BMDMs from wild-type (WT) mice as well as two mouse lines in which HDAC6 is either ablated (KO) (13) or contains a W1116A point mutation in the ZnF domain (ZnF^m, manuscript in preparation), which abolishes ubiquitin binding (10). BMDMs of the different genotypes were first primed by LPS and then challenged by nigericin, which activates the NLRP3 inflammasome by raising intracellular potassium (K^+) efflux (14) or MSU, which leads to generation of reactive oxygen species (ROS) through activation of NADPH oxidases (5). Inflammasome activation was monitored by examining the cleaved Caspase-1 p20 fragment by immunoblotting and by measuring release of the cytokine IL-1β in the culture supernatant (Fig. 1A). As shown in Figure 1B and 1C, generation of Caspase-1 p20 and production of IL-1β were similar in WT, KO and ZnF^m cells. The inflammasome dependence of the IL-1β release was confirmed by using the specific NLRP3 inhibitor MCC950 (16). Because strong inflammasome activation eventually leads to cell membrane damage and release of cellular contents, we examined cellular toxicity by measuring the level of lactate dehydrogenase (LDH) release from cells. Also in this case, the differences between the genotypes were minimal and did not reach statistical significance (Fig. 1D); thus, deletion or mutation of HDAC6 in primary BMDMs does not appear to protect cells from cell death. We next examined the kinetic of IL-1β release in BMDMs of the different genotypes. Interestingly, the IL-1β amount in HDAC6 KO and ZnF^m BMDMs reached a plateau rapidly in only 15 mins after nigericin challenge, while WT BMDMs responded to stimulation more slowly (Fig. S1). At later time points (between 30 and 90 mins), the IL-1β difference between the three BMDMs types were less significant, although the ZnF^m BMDMs showed a slightly reduced level. Collectively, our results in primary BMDMs did not demonstrate a clear dependency on HDAC6 or its ZnF domain for NLRP3 inflammasome activation, but indicate that HDAC6 may participate in the early timepoint response.

A ZnF-specific DARPin moderately inhibits NLRP3 inflammasome activation in THP-1 cells

To investigate more broadly the role of the HDAC6 ZnF in NLRP3 inflammasome activation, we switched from primary BMDMs to the leukemic THP-1 monocyte/macrophage cell line, a widely used surrogate for human monocytes or macrophages. We recently reported a synthetic protein based on a designed ankyrin repeat protein (DARPin) scaffold, DARPin F10, which can selectively bind to the HDAC6 ZnF Ub binding pocket in cells and blocks Ub recruitment (15) (Fig. 2A). We previously showed that DARPin F10 is highly specific for the HDAC6 ZnF (15). We had made a degradable version of DARPin F10 by fusing it to the $FKBP^{F36V}$ degron tag (16) and showed that it is efficiently degraded in A549 cells upon addition of the chemical dTAG-13 (hereafter dTAG). We used this system to generate THP-1 cells expressing DARPin F10 (F10-$FKBP^{F36V}$ THP-1 cells) and found that the protein was well-expressed and could be efficiently degraded within 6 hours of dTAG addition (Fig. 2B); furthermore, expression of DARPin F10 does not alter the level of endogenous HDAC6, or of the major class I HDACs, HDAC1 and 2 (Fig. S2A). Nigericin-induced NLRP3 activation was comparable in dTAG treated parental (WT) THP-1 cells (Fig. 2C) and in control cells expressing only the $FKBP^{F36V}$ moiety ($FKBP^{F36V}$ THP-1 cells, Fig. S2B), thus excluding a possible inhibitory effect of $FKBP^{F36V}$ expression or dTAG on IL-1β release. When parental WT THP-1 cells were treated with MCC950 (17), or CGP084892, a Caspase-1 inhibitor (18), IL-1β release was strongly reduced, as expected. A modest reduction of IL-1β secretion was observed in F10-$FKBP^{F36V}$ THP-1 cells, when compared to the WT THP-1 cells. Degradation of DARPin F10 by dTAG treatment led to a partial, but significant, recovery of IL-1β release (Fig. 2C). We next examined early timepoints - 0.5 and 1.5 hr post-nigericin activation - to study the impact of DARPin F10 on the kinetic of IL-1β release. In agreement with Figure 2C, we observed again a slight increase of IL-1β at 3.5 hr in dTAG-treated cells (Fig. 2D). However, a larger and significant difference was seen at 1.5 hr post activation. These data indicate that blockade of the HDAC6 ZnF domain moderately inhibits the NLRP3 inflammasome, particularly during the early phase of activation by nigericin in THP-1 cells.

HDAC6 degradation moderately inhibits NLRP3 inflammasome in PBMCs

Blocking specifically the ZnF domain in THP-1 cells by DARPin F10 showed a partial inhibition of NLRP3 inflammasome activation, confirming that HDAC6 contributes to this pathway. To extend these observations in other cell settings, we next made use of a novel HDAC6 proteolysis targeting chimera (PROTAC) degrader, XY-07-35 (19). Treatment of cells with XY-07-35 leads to recruitment of the E3 ligase cereblon (CRBN) to HDAC6, ubiquitination and subsequent proteasomal degradation of HDAC6 (Fig. 3A). This degrader is based on the HDAC inhibitor suberoylanilide hydroxamic acid (SAHA) fused by a linker to pomalidomide as a CRBN-binding moiety; the negative control compound XY-07-191 contains a methyl group on the pomalidomide moiety which disrupts CRBN recruitment (Fig. 3B). *In vitro* enzymatic assays with purified HDACs showed that XY-07-35 inhibited HDAC6 with a low IC_{50}=0.0485 μM, which is 10 times lower than for HDAC8 (0.621 μM) or other HDACs (1.04-5.75 μM; Fig. 3C); in addition, the degradation profile of XY-07-35 is highly specific for HDAC6 (19). This compound does not show cellular toxicity when tested over a broad concentration range in either HEK293T, Jurkat or U937 cells (Fig. S3A). We first tested the efficacy of XY-07-35 in immune cell lines. Unexpectedly, XY-07-35 treatment did not lead to HDAC6 degradation in both non-differentiated and PMA-differentiated THP-1 cells (Fig. S3B). Therefore, to assess its effect on NLRP3 inflammasome activation in human cells we used peripheral blood mononuclear cells (PBMCs). HDAC6 was efficiently degraded in PBMCs at 1 μM XY-07-35 concentration; by contrast, the negative control compound XY-07-191 or the IκKβ inhibitor AFN700 (18) had only minimal or no effect on HDAC6 levels (Fig. 3D). To test the functional consequence of HDAC6 degraders, PBMCs were first treated with the HDAC6 degrader or the negative control compound for 24 hrs, followed by LPS priming and subsequent stimulation with MSU, nigericin, or ATP to activate the NLRP3 inflammasome (Fig. 3E). The HDAC6 degrader XY-07-35 clearly reduced the IL-1β release under all stimulatory conditions as compared to DMSO, though partial inhibition was also seen with the negative control XY-07-191, suggesting some non-specific effects of the scaffold. HDAC6 degradation had the most profound inhibition of MSU-triggered IL-1β release, achieving ca. 60% of IL-1β reduction as compared to DMSO, while under nigericin and ATP stimulation, the reduction was 40%. A statistically significant reduction of IL-1β between XY-07-35 and the control compound XY-07-191, was only seen in the MSU conditions. Inhibitors of other nodes of the

pathway, the NLRP3 inflammasome inhibitor NP3-948 and AFN700 both led to an almost complete (>90%) inhibition of IL-1β release. The negative control compound XY-07-191 also minimally inhibited IL-1β release, but less effectively than XY-07-35, suggesting a beneficial effect of HDAC6 degradation. We also measured cell viability by using resazurin fluorescence in PBMCs, but since monocytes constitute only a minor fraction of the cell population, the pyroptosis could not be tracked efficiently. Overall, these results show partial reduction in NLRP3 inflammasome activation following degradation of HDAC6, with the magnitude of the effect depending on the stimulus.

HDAC6 degradation does not affect pyrin inflammasome activation

According to a previous report (11), activation of both NLRP3 and pyrin inflammasomes depends on HDAC6. To evaluate the importance of HDAC6 for the pyrin inflammasome, we used a previously established U937 pyrin-overexpressing cell line (20). In these cells, treatment with the bile acid derivative BAA473 activates the pyrin inflammasome, leading to the release of cytokines (e.g., IL-1β, IL-18) and pyroptosis; IL-18 expression is induced without the need for prior priming and was used for monitoring inflammasome activation. HDAC6 was efficiently degraded in the U937-pyrin expressing cells by XY-07-35 at concentrations ranging from 0.1 μM to 10 μM (Fig. 4A). However, treatment with XY-07-35 did not result in any change in IL-18 secretion compared to either DMSO control or the XY-07-191 control (Fig. 4B). Additionally, we measured cell viability and found that HDAC6 degradation by XY-07-35 did not protect cells from pyroptosis (Fig. S4), confirming that in this setting, HDAC6 degradation has no effect on pyrin inflammasome activation.

Discussion

In this study, we utilized a range of cellular systems and several orthogonal approaches to modulate HDAC6 activity and probe its role in NLRP3 and pyrin inflammasome activation. HDAC6 protein levels were modulated by both knock-out and chemically induced degradation, while function was probed by a knock-in unable to bind to ubiquitin and a DARPin inhibitor blocking ubiquitin recruitment. In contrast to a previous study reporting on the HDAC6-ubiquitin interaction as a crucial regulator of inflammasome activation (11), we did not observe a significant difference in NLRP3 inflammasome activation between WT and HDAC6 knock-out or HDAC6 ZnF^{m} (W1116A) BMDM cells. To investigate this further, we examined the effect of a small protein (DARPin F10) binding to the HDAC6 ZnF domain and preventing ubiquitin recruitment. This protein was shown to have a strong inhibitory impact on processes involving the ZnF-Ub interaction, such as the formation of aggresomes or stress granules, or infection by influenza or Zika virus (15). But under conditions of inflammasome induction, we observed only partial downregulation of IL-1β release in THP-1 cells expressing DARPin F10 when stimulated with nigericin. In primary PBMCs and U937 cells, the selective HDAC6 degrader XY-07-35 efficiently degraded HDAC6, but HDAC6 had only modest, stimulation-dependent effects on NLRP3 inflammasome activation. Furthermore, HDAC6 degradation had no effect on IL-18 release and pyroptosis mediated by pyrin. With respect to NLRP3 inflammasome activation, HDAC6 degradation had the strongest effect on MSU-stimulated IL-1β release, which is a milder, non-pyroptotic form of NLRP3 activation (Fig. 3E). Similarly, in THP1 cells, HDAC6 inhibition seemed to have its most pronounced effect at early timepoints. It is possible that HDAC6 plays a more pronounced role in response to crystalline inflammasome activators (in agreement with the results in Magupali et al, 2022). It has also been noted that other NLRP3 regulatory mechanisms such as PKD phosphorylation play an important role at early time points in cell culture experiments, but compensatory pathways override these effects at later timepoints (21).

Based on our results it seems that the importance of HDAC6 for NLRP3 inflammasome activation is not absolute, but condition and context dependent. On one hand, we noted that blocking the HDAC6 ZnF-Ub interaction with DARPin F10 in THP-1 cells and degrading HDAC6 in PBMCs both resulted in an inhibitory effect, thus

supporting a role for HDAC6 in this pathway. When degrading DARPin F10 with dTAG we only observed a partial rescue of IL-1β release; this can possibly be explained by incomplete degradation of DARPin F10, leading to some residual F10 (even in tiny amounts) that could interfere with ubiquitin recruitment. Similarly, incomplete HDAC6 clearance by the proteasome system might be responsible for the moderate downregulation of IL-1β release or cell death protection in XY-07-35 treated PBMCs. Furthermore, we found that the negative control compound XY-07-191 also exhibited slight inhibition of NLRP3 inflammasome activation, which we attribute to its possible catalytic inhibition of HDAC6. Indeed, both compounds are derived from SAHA (Fig. 3B), which is known to inhibit all HDACs including HDAC6, and previous studies have demonstrated that HDAC inhibition can downregulate IL-1β release (11, 22). Context dependence for HDAC6 inflammasome activation has also been observed in HDAC6 inhibitor studies. For instance, a recent study in THP-1 cells (23) showed that inhibiting HDAC6 by Tubastatin A leads to a reduced IL-1b release, but in another study in BMDMs (24), Tubastatinn A did not impact the mIL-1b level. We notice these differences and remark that current HDAC inhibitors, including HDAC6-selective inhibitors, may not be as specific as previously reported(25).

On the other hand, we found that the activation of the NLRP3 inflammasome in BMDMs from HDAC6 KO and ZnF^{m} (W1116A) mice took place normally; likewise, activation of the pyrin inflammasome in U937-pyrin cells was not affected by HDAC6 depletion. In a previous study using immortalized BMDMs (11), researchers described a HDAC6-mediated aggresome-like pathway for NLRP3 inflammasome formation, and reported that deletion of HDAC6 or mutations in the ZnF domain completely blocked inflammasome activation, in contrast to our results. Likewise, another recent study reported that the lysosomal Ragulator complex is important for NLRP3 inflammasome activation in vivo via interaction with HDAC6 (12).

We hypothesize that the partial discrepancy may result from the differences in the cell types and specific experimental conditions used. Immortalized cells are known to carry chromosomal abnormalities that allow them to proliferate indefinitely, leading to changes in their transcriptome, proteome and reliance on specific pathways compared to primary cells. As a result, it is reasonable to speculate that established iBMDMs may behave differently from primary BMDMs. As for the pyrin inflammasome, we used U937 cells instead of iBMDMs, and bile acid derivatives instead of Clostridioides

difficile toxin B (TcdB) to activate the pathway, which may also contribute to the observed differences in results obtained. In summary, we conclude that HDAC6 can participate in NLRP3 inflammasome activation, but its importance appears to be context dependent.

Experimental procedures

Cell Culture

THP-1, U937, PBMC and BMDM cells were cultured in Roswell Park Memorial Institute (RPMI) 1640 Medium–stable Glutamine (Bioconcept#1-41F03-1) supplemented with 10% fetal bovine serum (FBS). For BMDMs the medium also contained M-CSF 1 (100 ng/mL). All cells were cultured in 5% CO_2 at 37°C.

BMDMs isolation and culture

BMDMs were isolated as previously described (26). In short, mice (8~14 weeks old) were sacrificed and both legs were sterilized in 70% ethanol. Attached tissues were removed by dissection with scissors and the isolated bones were flushed or crushed twice in a mortar with 5 mL RPMI 1640 medium. The suspension from crushed bones was filtered through 100 µm cell strainer (Falcon#352360) to remove debris. Filtered cells were centrifuged at 500 x g, 15 mins at room temperature. Supernatant was removed and cell pellets were resuspended in RPMI 1640 (+M-CSF 1, 100 ng/mL). The cell suspension (from 1 leg) was divided into four Nunc Square 25-cm dishes (Thermo Scientific#166508), with each plate containing 10 mL cell suspension. On Day 3 post-seeding, 5 mL fresh RPMI 1640 (+M-CSF 1) medium was added to each plate. On Day 6, BMDMs were ready for collection or re-seeding for new experiments. All mice handling was done according to Swiss federal guidelines for animal experimentation and approved by the FMI Animal committee and the local veterinary authorities (Kantonales Veterinäramt of Kanton Basel-Stadt).

Immunoblotting

Treated BMDM cells were lysed with RIPA buffer (supplied with cOmplete™ Protease Inhibitor Cocktail, Merck#11697498001), and protein concentration was determined by Bradford assay. Same protein amounts were loaded onto 4-12% NuPAGE Gels

and protein was transferred to PVDF membranes by using Trans-Blot® Turbo™ Transfer System (Biorad#17001917). Membrane was blocked with 5% milk-TBS, and then incubated with primary antibodies overnight at 4°C. Signal was developed with HRP-conjugated secondary antibodies and Amersham ECL Western Blotting Detection Reagent (Cytiva#RPN2106). Antibody information: mouse Caspase-1 (p20) (AdipoGen#AG-20B-0042-C100), mHDAC6 (homemade), human HDAC6 (CellSignaling#7558), α-tubulin (Sigma-Aldrich #T9026), HA (CellSignaling#3724), pan Actin (Sigma-Aldrich#SAB4502632).

ELISA (for IL-1β and IL-18)

Supernatant from treated cells were collected and frozen at -80°C before determining cytokine concentrations. mIL-1β was determined by ELISA MAX™ Standard Set Mouse IL-1β kit (BioLegend# 432601). Human IL-1β and IL-18 were determined with Cisbio HTRF Cisbio Human IL1β (#62HIL1BPET) and Human IL18 (#62HIL18PEG) protocols. All the data were from 3 or 4 independent biological replicates.

LDH measurement

Culture supernatants from the different BMDMs samples were analyzed with the CytoTox 96® Non-Radioactive Cytotoxicity Assay Kit (Promega# G1780). Total cell lysate of non-treated (i.e., DMSO only -no inhibitor-, but induced for inflammasome formation) BMDM cells was defined as 100% cell death or cytotoxicity. Values from other conditions were calculated as follows: $(OD_{\text{treated cells}}-OD_{\text{no-inhibitor control}})\div(OD_{\text{total lysate}}-OD_{\text{no-inhibitor control}}) * 100$.

Single cell clonal THP-1 F10 and FKBP cells establishment

Lentiviral vectors for HA-DARPin F10-FKBP^{F36V} and HA-FKBP^{F36V} was from previous work (15). Lentivirus was generated with 3rd generation lentivirus packaging systems. In detail, DARPin F10 vector and lentivirus packaging plasmids (Tat, Rev, Gag/pol, Vsv-g) were co-transfected in 293T cells in 6 well-plates. After 3 days culturing, supernatants were harvested and concentrated with Lenti-X™ Concentrator (Takara# 631232). Virus pellet was resuspended in 1~4 mL RPMI1640 medium (with 10% FBS). Next, THP-1 cells were seeded in 6 well-plates (each well with 1 x10^6 cells), and then lentivirus was added to the plate in the presence of polybrene (8 μg/mL), followed by

centrifugation at 1500 rpm / 453 x g, for 45 mins at room T°. After transduction, THP-1 cells were cultured at 37°C for 7~14 days. The cell number and density were monitored carefully; when a concentration of > 2 x10^6 cells per mL was reached, 2 µg/mL puromycin was added for selection for 3~6 days. Surviving cells were single cell sorted by FACS into 96 well plates (in RPMI1640 without puromycin). After about 1 month in culture, single cell clones were analyzed by immunoblotting to test for DARPin F10 expression. Cell clones with a good expression level were stored in cryo-solution (90% FBS + 10% DMSO) in liquid nitrogen.

Inflammasome activation

For BMDM cells, 1.5 x10^6 cells per well were seeded in 6 well-plates. After priming with 1 µg/ml LPS (Invivogen #tlrl-b5lps), cells were challenged with 200 µg/ml MSU crystals (Invivogen #tlrl-msu-25) for 6 hours or 20 µM nigericin (Sigma-Aldrich #N7143-5MG) for 30 mins. For THP-1 cells, 5x10^5 cells/mL were primed with 0.5 µM PMA (Invivogen #tlrl-pma) in T75 Ultra-low binding flask (CORNING #3814) for 3 hours, and then cells were collected by centrifugation at 500 x g, for 5 mins. The supernatant was removed, and fresh medium was added to have cells at a density of around 5x10^5 cells/mL. 100 µL cells were seeded in 96 well plate and incubated for 1~2 days. During the culturing, dTAG was added when needed to degrade the DARPin. After 1~2 days culturing, inflammasome was activated by adding 15 µM nigericin for up to 4 hours. For PBMCs, 3x10^4 cells per were seeded, and primed with 0.2 ng/mL LPS for 4 hours and then incubated with MSU 200 µg/mL (5 hours), nigericin 2 µM (2 hours) or ATP 3 mM (0.5 hours). For pyrin inflammasome, U937-pyrin cells were seeded in 96 well after 0.5 µM PMA treatment for 3 hours and then challenged by BAA473 (200 µM) for 4 hrs at 37°C. For control experiments inhibitors were used at the following final concentration: MCC950 at 10 µM, CGP084892 at 20 µM. NP3-948 is a potent NLRP3 inhibitor developed at Novartis that competes with MCC950 for binding to the NLRP3 protein (27).

Cell viability Assay

Cell viability of PBMCs and U937 cells was checked with PrestoBlue™ HS Cell Viability Reagent (Invitrogen # P50200) according to the manufacturer's instructions.

After incubation for 1 to 2 hrs, fluorescence was determined with a PheraStar plate reader under Ex/Em=540/590 nm.

Cell viability with CTG assay

U937, Jurkat, and HEK293T cells were plated with a density of 10^5 cells/mL, with 50 µL/ well in a white 384 well plate (Corning #3570). Two hours after plating, XY-07-035 was dispensed to each well using HPd300e and incubated at 37℃ for 70 hours. CellTiter-Glo® (CTG) Luminescent Cell Viability Assay (Promega #G7572) was then used to measure cell viability. Aliquoted frozen CTG reagent and cell plates were warmed to room temperature prior to loading. After the plates were cooled to room temperature, the CTG reagent was loaded 15 µL/ well with an electronic multichannel pipette. To ensure the reagent had fully reacted with cells, plates were centrifuged at 500 g, 3 min followed by a 30 min incubation in a dark box at room temperature. The luminescence signal was read over 10 cycles for each data point on a PHERAstar FS microplate reader (BMG Labtech). The Relative abundance was calculated as the sum of the averages of duplicate individual 12-point dose-response data points.

Statistical analysis

All the statistical analysis were done with One-way or Two-way ANOVA test, corrected for multiple comparisons using post-hoc significance Tukey test. A significance level of $p < 0.05$ was used.

Data availability

Mass spectrometry data related to HDAC6 degrader XY-07-35 and XY-07-191 are deposited to PRIDE under archive number PXD023652. The data that supports the findings described in this work are available from the corresponding author upon request.

Acknowledgements and funding

We thank Christelle Arnold (NIBR) for her help in setting up the collaboration with FMI. We also thank Chun Cao and Gabriele Matthias for maintaining and providing HDAC6 KO and ZnF^m mice. Financial support through the SystemsX.ch MRD project VirX

2014/264, evaluated by the Swiss National Science Foundation, and by the European Research Council ERC Synergy grant number 856581 CHUbVi is gratefully acknowledged. RK was supported by the European Union's Horizon 2020 research and innovation program under the Marie Sklodowska-Curie grant agreement No 894690. This work was supported by the Novartis Research Foundation. This work was supported by the National Institutes of Health (NIH) grant R01CA262188 (to E.S.F.).

Authors contributions

L.W. performed most of the experiments in BMDMs, THP-1 F10 cells, analysis, preparation of figures and wrote the manuscript draft. S.S performed the revised experiments and helped with the revised manuscript writing. R.K helped with BMDMs isolation and culture, and with manuscript modifications. X.Y., K.A.D., C.L.H. and E.S.F. were responsible for providing the HDAC6 degrader and corresponding characterization, and manuscript proofreading. S.G and J.S. helped with DARPin experiment. F.B. led the collaboration between NIBR and FMI, and helped with experimental design and manuscript preparation, A.U. was responsible for the experiments in PBMCs and U937-pyrin cells, and for measuring IL-1β in various samples, S.A. performed the HDAC6 degrader experiments in THP-1 and U937 cells, C.J.F. was responsible for experimental design, conceptualization, and manuscript preparation. P.M was responsible for the conceptualization, supervision, writing the original draft and review, project administration and funding acquisition. All authors contributed to the final manuscript.

Declaration of interests

Part of the results presented herein have been used in the patent application EP-A-20213494.6. A.U., S.A., C.J.F. and F.B. are employees of Novartis. E.S.F is a founder, scientific advisory board (SAB) member, and equity holder of Civetta Therapeutics, Lighthorse Therapeutics, Proximity Therapeutics, and Neomorph, Inc. (also board of directors). He is an equity holder and SAB member for Avilar Therapeutics and Photys Therapeutics and a consultant to Novartis, Sanofi, EcoR1 Capital, Ajax Therapeutics, Odyssey Therapeutics and Deerfield. The Fischer lab receives or has received

research funding from Deerfield, Novartis, Ajax, Interline and Astellas. K.A.D is a consultant to Kronos Bio and Neomorph Inc.

Figure Legends

Figure 1: The NLRP3 inflammasome is activated normally in HDAC6 KO or ZnF^{m} primary mouse BMDMs

(A) Workflow for evaluating NLRP3 inflammasome activation in BMDMs. Bone marrow was isolated from mice strains with different mutations in HDAC6 as indicated and BMDMs were expanded for 7 days in the presence of M-CSF1. Subsequently, BMDMs were primed for 4 hrs with LPS (1 µg/mL) and NLRP3 inflammasome formation was induced by nigericin (20 µM) or MSU (200 µg/mL) addition. Release of IL-1β was monitored by ELISA and activation/cleavage of Caspase-1 was evaluated by immunoblotting.

(B) Normal NLRP3 activation in WT, HDAC6 KO and HDAC6 ZnF^{m} BMDMs. Immunoblot monitoring HDAC6, Capase-1 (p20) cleavage and α-tubulin as loading control. Nigericin and MSU were used with LPS primed BMDMs (n = 3).

(C) Normal mIL-1β release in the supernatant from WT, HDAC6 KO and ZnF^{m} BMDMs. IL-1β from supernatant in (B) was measured by ELISA and statistical analysis was done with one-way ANOVA. ns, no significant difference.

(D) No difference in cytotoxicity following inflammasome induction in WT, HDAC6 KO and ZnF^{m} BMDMs. Lactate dehydrogenase (LDH) was measured in the culture supernatant from (B) and statistical analysis was done by one-way ANOVA. ns, no significant difference.

Figure 2: A DARPin blocking the HDAC6-Ub interaction has a modest effect on IL-1β release from THP-1 cells

(A) Structure of the DARPin F10 - HDAC6 ZnF domain complex (PDB: 7ZYU) showing blockade of Ub recruitment. The surface representation shows HDAC6 ZnF (yellow) and the C-terminal LRGG of Ub (light pink) (overlayed with PDB:3GV4), the ribbon representation depicts DARPIN F10 (cyan).

(B) Establishment of a THP-1 F10-FKBP cell line with degradable DARPin F10. Immunoblotting with lysates of THP-1 F10-FKBP cells treated at the indicated concentration with dTAG (for 6 hrs). The leftmost lane (WT) shows the parental THP-1 cells. The membrane was probed with antibodies against actin as loading control and F10 (HA-F10-FKBP ^{F36V}, detected with anti-HA).

(C) IL-1β release under various treatments in THP-1 F10-FKBP cells at 3 hrs post-nigericin stimulation. Cells were treated as indicated in the scheme at the top. The graph at the bottom shows the measurement of IL-1β in cell supernatants, based on 3 independent experiments. MCC950 and CGP084892 are NLRP3 and Caspase-1 inhibitors, respectively. One-way ANOVA test was applied for statistical analysis. ****, $p<0.0001$. Cells were first treated with PMA (0.5 μM) for 3 hrs, then medium was exchanged and dTAG was added (1 μM); MCC950 (10 μM) and CGP084892 were added 30 mins before nigericin (15 μM) treatment.

(D) IL-1β release from 0 hr to 3.5 hrs after nigericin treatment in THP-1 or THP-1-F10-FKBP cells. Experimental set-up was as in (B) and IL-1β concentration was monitored at timepoint 0, 0.5, 1.5, and 3.5 hrs post nigericin treatment. Two-way ANOVA tests were applied, and comparison was performed within each timepoint between with and without dTAG group. **, $p<0.01$. Experimental setup as in (C).

Figure 3: Effect of XY-07-35 mediated HDAC6 degradation on NLRP3 inflammasome activation in PBMCs

(A) Schematic of the mode of action of an HDAC6 degrader. The PROTAC engages both HDAC6 and the E3 ligase cereblon (CRBN), which then leads to ubiquitination and degradation of HDAC6.

(B) Chemical structure of the HDAC6 degrader XY-07-35 and of the negative control XY-07-191 which no longer recruits CRBN.

(C) *In vitro* enzymatic assay of compound XY-07-35 on the activity of different HDACs. IC_{50} for each enzyme is shown.

(D) XY-07-35 mediated HDAC6 degradation in PBMCs. PBMCs (without or with LPS priming for 4 hrs) were treated with the indicated compounds and HDAC6 levels were detected by immunoblotting with an anti-HDAC6 antibody. Detection of actin was used as control for loading. CGP, CGP084892 (Caspase-1 inhibitor); AFN700 is an inhibitor of the NF-kB pathway (IKK inhibitor).

(E) HDAC6 degradation impact on IL-1β release in PBMCs following MSU 200 μg/mL (5 hrs), nigericin 2 μM (2 hrs) or ATP 3 mM (0.5 hrs) treatment. Cells were first primed with 0.2 ng/mL LPS for 4 hrs at 37°C, then treated with MSU, nigericin and ATP as indicated. The graphs below show the results of 3 independent experiments using the inducers as indicated. NP3-948 is an inhibitor of the NLRP3 inflammasome.

Figure 4: Effect of HDAC6 degradation on pyrin inflammasome activation in U937 cells
(A) XY-07-35 mediated HDAC6 degradation in pyrin-expressing U937 cells. Cells were treated with the indicated compounds and HDAC6 was detected by immunoblotting with an anti-HDAC6 antibody. Detection of actin was used as a control for protein loading.

(B) No impact of HDAC6 degradation on IL-18 release in U937-pyrin cells treated with the indicated compounds. Pyrin inflammasome was activated by BAA473 (200 μM) for 4 hrs at 37°C. The scheme at the top depicts the experimental outline. The graph at the bottom presents IL-18 release based on 4 independent experiments. CGP, CGP084892 (200 μM).

Supporting information

Figure S1 (related to Fig. 2):
BMDM cells were primed by LPS (1 μg/mL) for 4 hrs and then challenged with 20 μM nigericin. 50 μL supernatant was collected every 15 mins (up to 90 mins) and mIL-1β level was determined by HTRF assay. Two-Way ANOVA test was used to compare the difference between each mouse line (WT, HDAC6 KO and HDAC6 ZnF^{m}) at each timepoint. p values between KO and WT, or ZnF^{m} and WT are presented as: *, $p<0.05$; **, $p<0.01$; ****, $p<0.0001$; ns, no significant difference.

Figure S2 (related to Fig. 3):
(A) Immunoblot of HDAC1, HDAC2 and HDAC6 protein level in WT THP-1 cells vs DMSO or dTAG treated F10-$FKBP^{F36V}$ THP-1 cells. DARPin F10 was detected by anti-HA antibody.

(B) $FKBP^{F36V}$ THP-1 cells were established for evaluating the possible effect of dTAG on IL-1β release. Cells were first treated with PMA (0.5 μM) for 3 hrs, then medium was changed and vehicle or dTAG was added (1 μM), followed by 20 μM nigericin for 3 hrs.

Figure S3 (related to Fig. 3):

(A) CTG cell viability assay to analyze degrader XY-07-035 toxicity in HEK293T, Jurkat and U937 cells. Cells were treated with different concentrations of the degrader, and cell viability determined by CTG assay was normalized to the non-treated group. Scale bar is presented as mean ±SD.

(B) THP-1 cells, with or without in vitro differentiation, were incubated with XY-07-35 and the HDAC6 level was examined by immunoblotting.

Figure S4 (related to Fig. 4):

Cell viability was measured by resazurin assay, and fluorescence intensity was a representative of the viability. No significant difference was found among DMSO, XY-07-35 and XY-07-191 groups. Maximum survival was obtained when cells were treated with the inflammasome inhibitor CGP.

References

1. Mariathasan, S., Newton, K., Monack, D. M., Vucic, D., French, D. M., Lee, W. P. *et al.* (2004) Differential activation of the inflammasome by caspase-1 adaptors ASC and Ipaf Nature **430**, 213-218 10.1038/nature02664
2. Broz, P., andDixit, V. M. (2016) Inflammasomes: mechanism of assembly, regulation and signalling Nat Rev Immunol **16**, 407-420 10.1038/nri.2016.58
3. Swanson, K. V., Deng, M., andTing, J. P. (2019) The NLRP3 inflammasome: molecular activation and regulation to therapeutics Nat Rev Immunol **19**, 477-489 10.1038/s41577-019-0165-0
4. Perregaux, D., andGabel, C. A. (1994) Interleukin-1 beta maturation and release in response to ATP and nigericin. Evidence that potassium depletion mediated by these agents is a necessary and common feature of their activity The Journal of biological chemistry **269**, 15195-15203,
5. Martinon, F., Pétrilli, V., Mayor, A., Tardivel, A., andTschopp, J. (2006) Gout-associated uric acid crystals activate the NALP3 inflammasome Nature **440**, 237-241 10.1038/nature04516
6. Jennifer A. Johnston, C. L. W., and Ron R. Kopito (1998) Aggresomes: A Cellular Response to Misfolded Proteins The Journal of Cell Biology, **143**, 1883-1898,
7. Kawaguchi, Y., Kovacs, J., McLauri, A., Vance, J., Ito, A., andYao, T. (2003) The Deacetylase HDAC6 Regulates Aggresome Formation and Cell Viability in Response to Misfolded Protein Stress Cell **Vol. 115, 727–738**,
8. Saito, M., Hess, D., Eglinger, J., Fritsch, A. W., Kreysing, M., Weinert, B. T. *et al.* (2019) Acetylation of intrinsically disordered regions regulates phase separation Nat Chem Biol **15**, 51-61 10.1038/s41589-018-0180-7
9. Rodriguez-Gonzalez, A., Lin, T., Ikeda, A. K., Simms-Waldrip, T., Fu, C., andSakamoto, K. M. (2008) Role of the aggresome pathway in cancer: targeting histone deacetylase 6-dependent protein degradation Cancer Res **68**, 2557-2560 10.1158/0008-5472.Can-07-5989
10. Indranil Banerjee, Y. M., Samuel Philip Nobs, Christoph Schneider, Peter Horvath, Manfred Kopf, Patrick Matthias, Ari Helenius, Yohei Yamauchi (2014) Influenza A virus uses the aggresome processing machinery for host cell entry Science **346**, 473-477,
11. Magupalli, V., Negro, R., Tian, Y., Hauenstein, A., Di Caprio, G., Skillern, W. *et al.* (2020) HDAC6 mediates an aggresome-like mechanism for NLRP3 and pyrin inflammasome activation Science **369**, eaas8995 10.1126/science.aas8995
12. Tsujimoto, K., Jo, T., Nagira, D., Konaka, H., Park, J. H., Yoshimura, S. I. *et al.* (2023) The lysosomal Ragulator complex activates NLRP3 inflammasome in vivo via HDAC6 The EMBO journal **42**, e111389 10.15252/embj.2022111389
13. Zhang, Y., Kwon, S., Yamaguchi, T., Cubizolles, F., Rousseaux, S., Kneissel, M. *et al.* (2008) Mice lacking histone deacetylase 6 have hyperacetylated tubulin but are viable and develop normally Mol Cell Biol **28**, 1688-1701 10.1128/mcb.01154-06
14. Muñoz-Planillo, R., Kuffa, P., Martínez-Colón, G., Smith, B. L., Rajendiran, T. M., andNúñez, G. (2013) K^+ efflux is the common trigger of NLRP3 inflammasome activation by bacterial toxins and particulate matter Immunity **38**, 1142-1153 10.1016/j.immuni.2013.05.016

15. Wang, L., Moreira, E. A., Kempf, G., Miyake, Y., Oliveira Esteves, B. I., Fahmi, A. *et al.* (2022) Disrupting the HDAC6-ubiquitin interaction impairs infection by influenza and Zika virus and cellular stress pathways Cell reports **39**, 110736 https://doi.org/10.1016/j.celrep.2022.110736
16. Natsume, T., andKanemaki, M. T. (2017) Conditional Degrons for Controlling Protein Expression at the Protein Level Annu Rev Genet **51**, 83-102 10.1146/annurev-genet-120116-024656
17. Coll, R. C., Robertson, A. A., Chae, J. J., Higgins, S. C., Muñoz-Planillo, R., Inserra, M. C. *et al.* (2015) A small-molecule inhibitor of the NLRP3 inflammasome for the treatment of inflammatory diseases Nat Med **21**, 248-255 10.1038/nm.3806
18. Unterreiner, A., Rubert, J., Kauffmann, M., Fruhauf, A., Heiser, D., Erbel, P. *et al.* (2021) Pharmacological inhibition of IKKβ dampens NLRP3 inflammasome activation after priming in the human myeloid cell line THP-1 Biochem Biophys Res Commun **545**, 177-182 10.1016/j.bbrc.2021.01.051
19. Xiong, Y., Donovan, K. A., Eleuteri, N. A., Kirmani, N., Yue, H., Razov, A. *et al.* (2021) Chemo-proteomics exploration of HDAC degradability by small molecule degraders Cell Chem Biol **28**, 1514-1527.e1514 10.1016/j.chembiol.2021.07.002
20. Alimov, I., Menon, S., Cochran, N., Maher, R., Wang, Q., Alford, J. *et al.* (2019) Bile acid analogues are activators of pyrin inflammasome The Journal of biological chemistry **294**, 3359-3366 10.1074/jbc.RA118.005103
21. Heiser, D., Rubert, J., Unterreiner, A., Maurer, C., Kamke, M., Bodendorf, U. *et al.* (2021) Evaluation of protein kinase D auto-phosphorylation as biomarker for NLRP3 inflammasome activation PloS one **16**, e0248668 10.1371/journal.pone.0248668
22. Xu, J., Zhao, X., Jiang, X., He, L., Wu, X., Wang, J. *et al.* (2022) Tubastatin A Improves Post-Resuscitation Myocardial Dysfunction by Inhibiting NLRP3-Mediated Pyroptosis Through Enhancing Transcription Factor EB Signaling J Am Heart Assoc **11**, e024205 10.1161/jaha.121.024205
23. Bockstiegel, J., Wurnig, S. L., Engelhardt, J., Enns, J., Hansen, F. K., andWeindl, G. (2023) Pharmacological inhibition of HDAC6 suppresses NLRP3 inflammasome-mediated IL-1β release Biochem Pharmacol **215**, 115693 10.1016/j.bcp.2023.115693
24. Hwang, I., Lee, E., Jeon, S.-A., andYu, J.-W. (2015) Histone deacetylase 6 negatively regulates NLRP3 inflammasome activation Biochemical and Biophysical Research Communications **467**, 973-978 https://doi.org/10.1016/j.bbrc.2015.10.033
25. Lechner, S., Malgapo, M. I. P., Gratz, C., Steimbach, R. R., Baron, A., Ruther, P. *et al.* (2022) Target deconvolution of HDAC pharmacopoeia reveals MBLAC2 as common off-target Nat Chem Biol 10.1038/s41589-022-01015-5
26. Afroz, S. F., Condon, N. D., Sweet, M. J., andKapetanovic, R. (2022) Quantifying Regulated Mitochondrial Fission in Macrophages Methods Mol Biol **2523**, 281-301 10.1007/978-1-0716-2449-4_18
27. Dekker, C., Mattes, H., Wright, M., Boettcher, A., Hinniger, A., Hughes, N. *et al.* (2021) Crystal Structure of NLRP3 NACHT Domain With an Inhibitor Defines Mechanism of Inflammasome Inhibition J Mol Biol **433**, 167309 10.1016/j.jmb.2021.167309

Figure 1

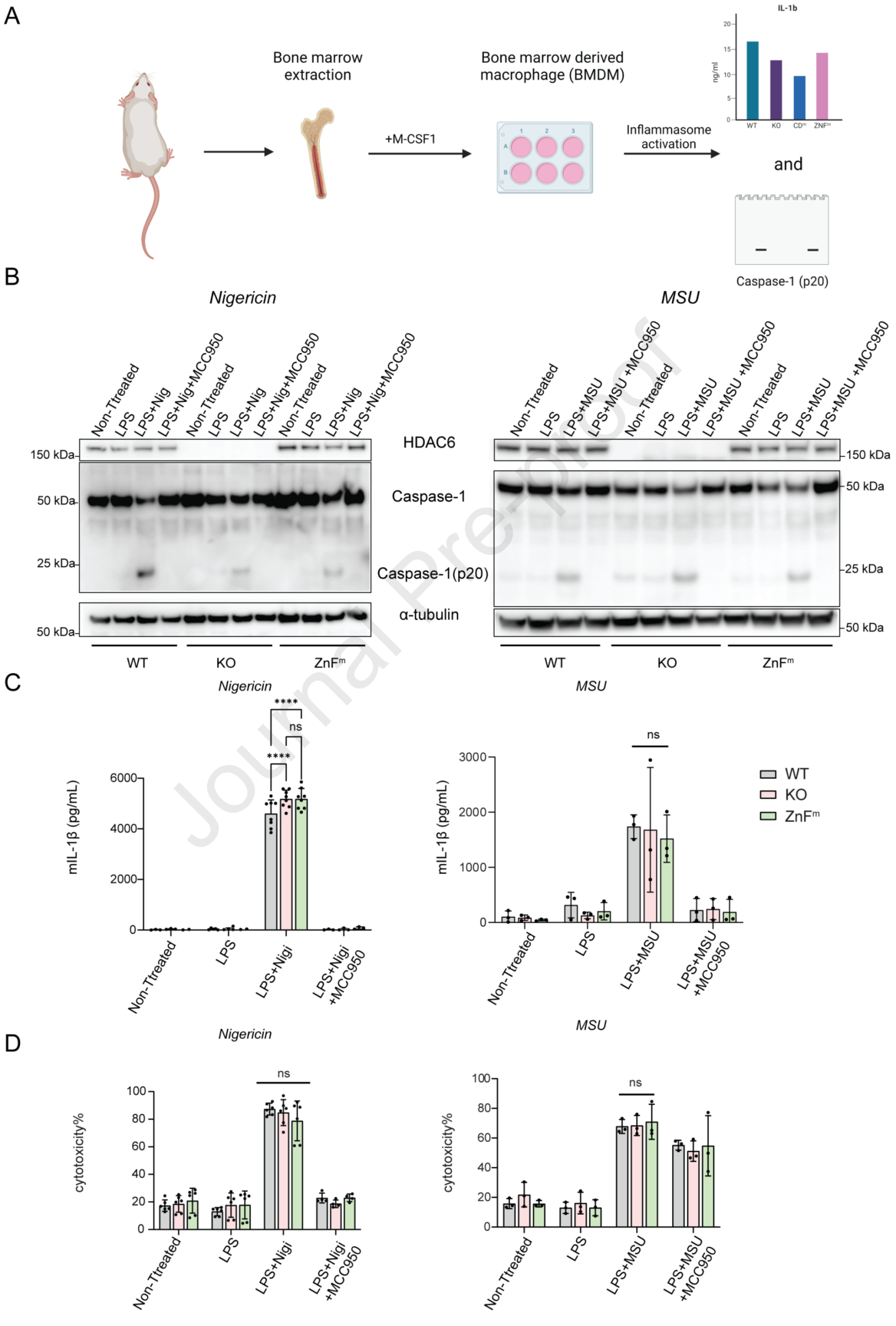

Figure 2

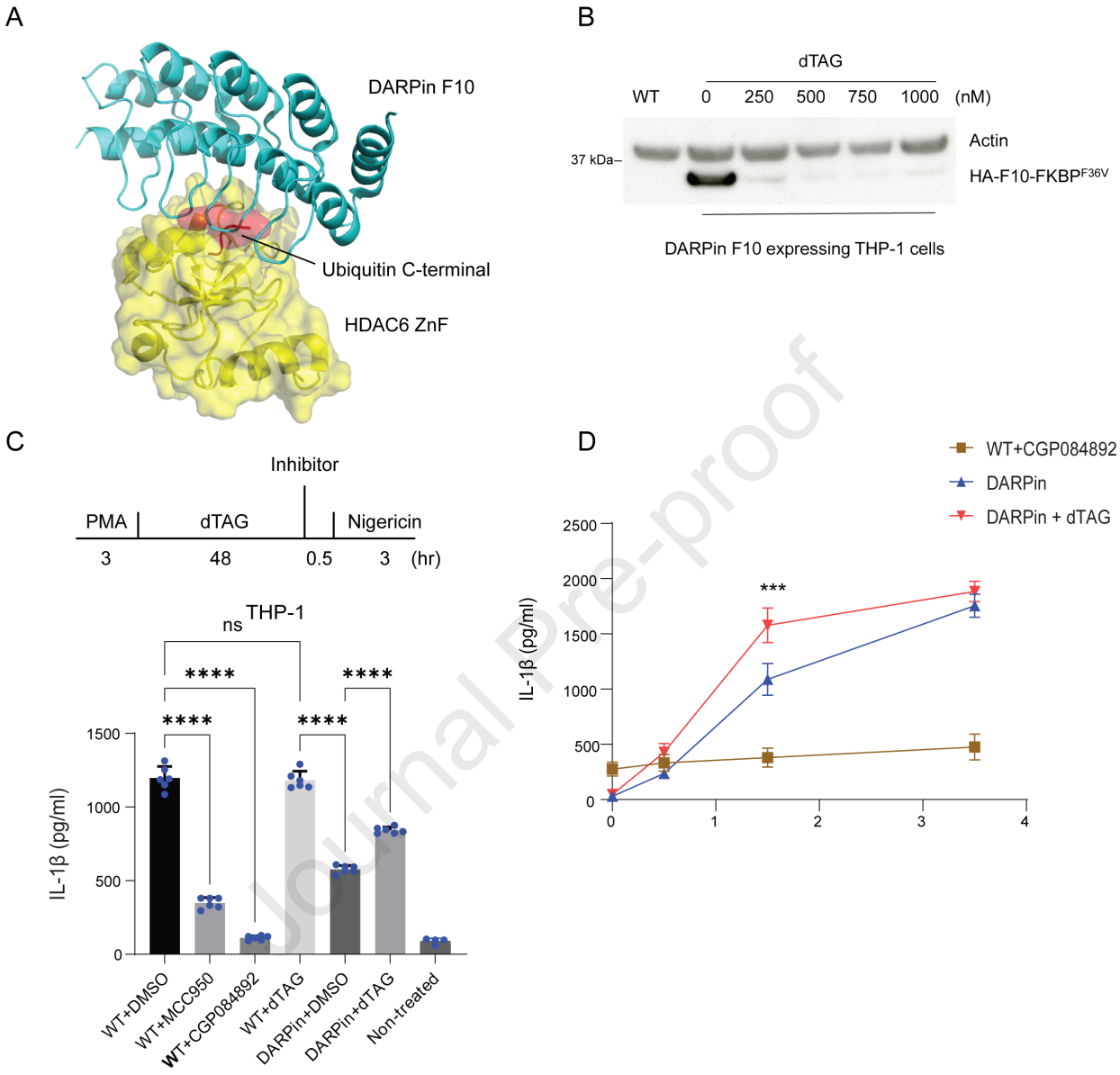

Figure 3

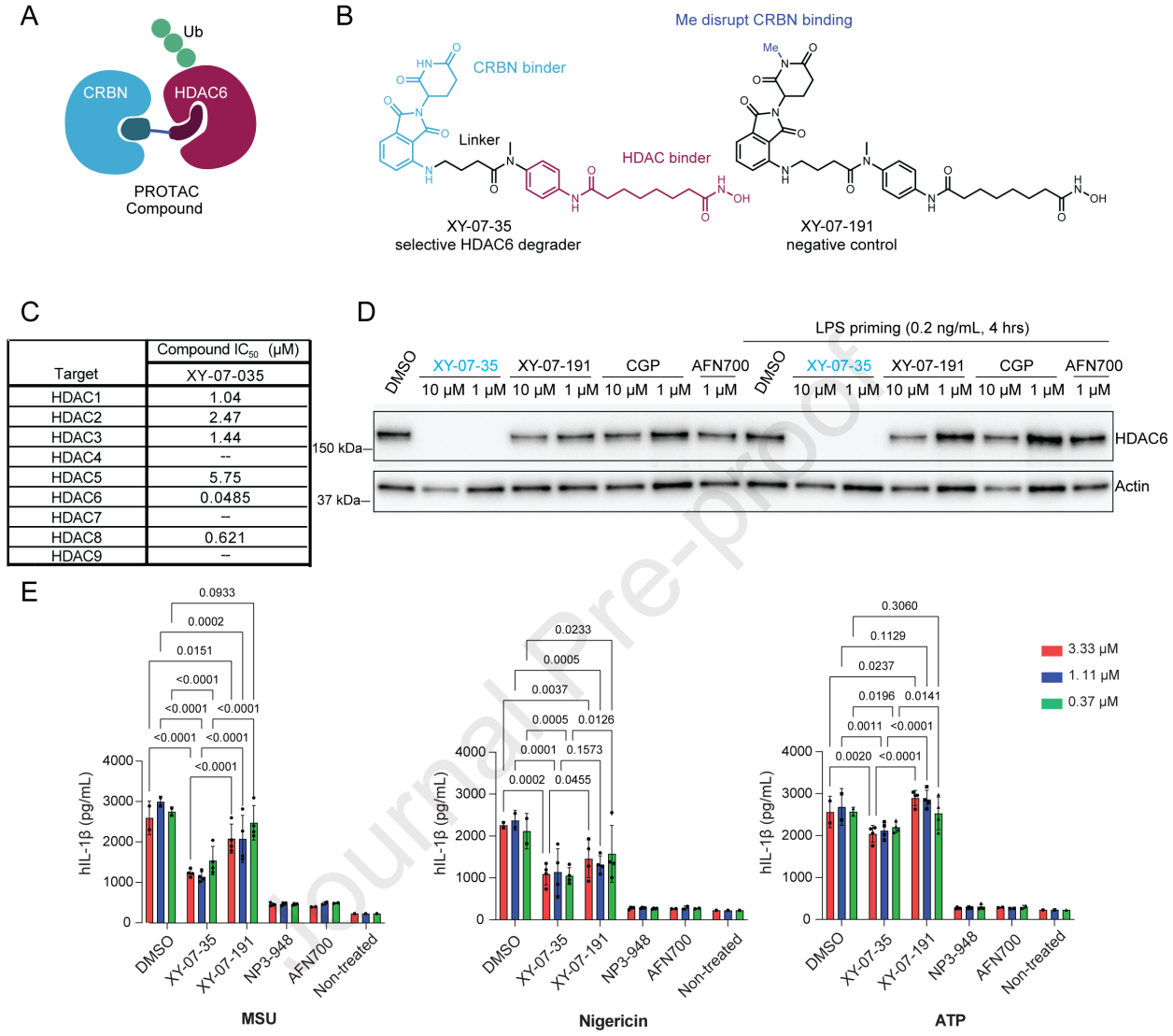

Target	Compound IC_{50} (μM) XY-07-035
HDAC1	1.04
HDAC2	2.47
HDAC3	1.44
HDAC4	--
HDAC5	5.75
HDAC6	0.0485
HDAC7	--
HDAC8	0.621
HDAC9	--

Figure 4

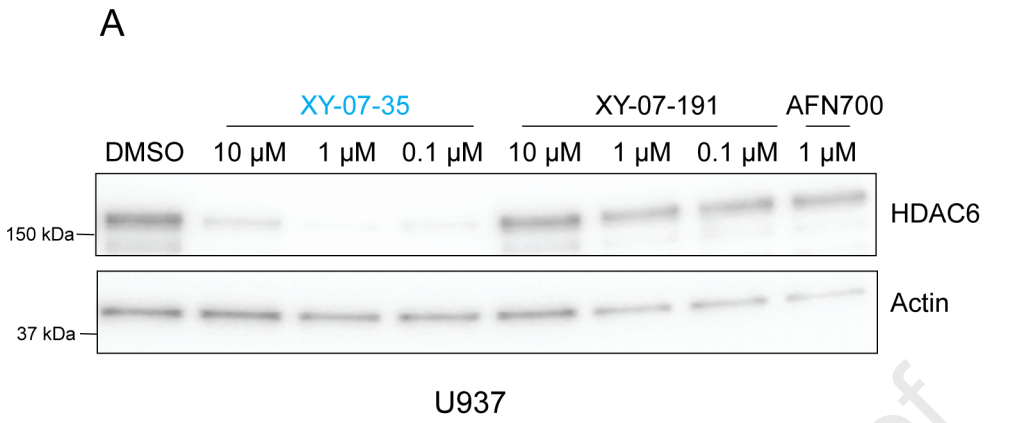

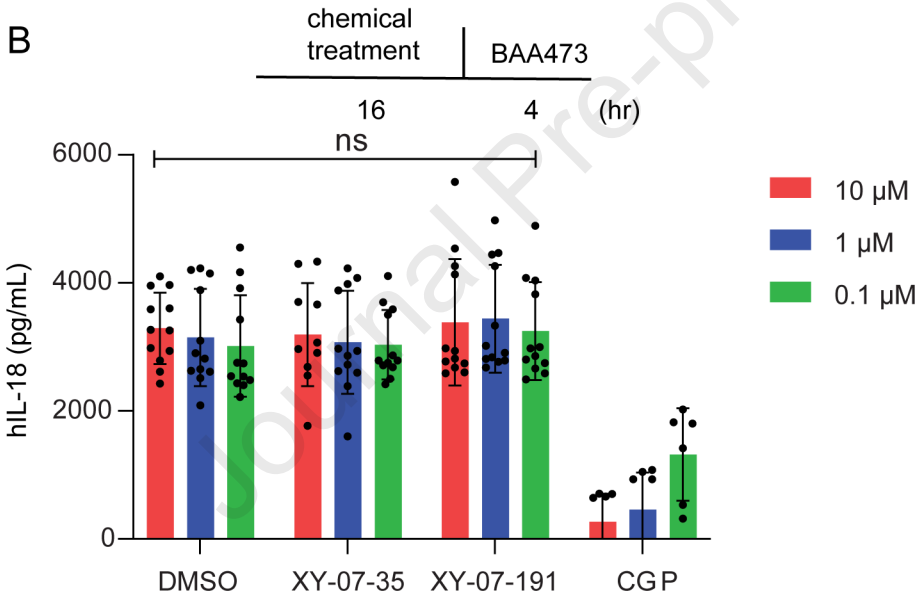

Author CRediT Statement

Longlong Wang: Conceptualization, Methodology, Software, Validation, Formal analysis, Investigation, Writing - Original Draft, Visualization. **Shihua Shi**: Software, Validation, Formal analysis, Investigation, Writing – Review & Editing. **Adeline Unterreiner**: Methodology. **Ronan Kapetanovic**: Methodology, Investigation, Writing - Original Draft. **Sucheta Ghosh**: Validation, Writing – Review & Editing. **Jacint Sanchez**: Validation, Writing – Review & Editing. **Selma Aslani**: Investigation. **Yuan Xiong**: Investigation, Resource. **Chi-Lin Hsu**: Investigation, Resource. **Katherine A. Donovan**: Investigation, Resource. **Christopher J. Farady**: Resource, Writing - Original Draft. **Eric S. Fischer**: Resource, Writing - Original Draft. **Frédéric Bornancin**: Resource, Conceptualization, Writing-Original Draft. **Patrick Matthias**: Conceptualization, Writing - Original Draft, Supervision, Project administration, Funding acquisition.

Declaration of interests

Part of the results presented herein have been used in the patent application EP-A-20213494.6. E.S.F is a founder, scientific advisory board (SAB) member, and equity holder of Civetta Therapeutics, Lighthorse Therapeutics, Proximity Therapeutics, and Neomorph, Inc. (also board of directors). He is an equity holder and SAB member for Avilar Therapeutics and Photys Therapeutics and a consultant to Novartis, Sanofi, EcoR1 Capital, Ajax Therapeutics, Odyssey Therapeutics and Deerfield. The Fischer lab receives or has received research funding from Deerfield, Novartis, Ajax, Interline and Astellas. K.A.D is a consultant to Kronos Bio and Neomorph Inc.